2012

Transcription factor Olig2 defines subpopulations of retinal progenitor cells biased toward specific cell fates

Brian P. Hafler, *Harvard Medical School*
Natalia Surzenko, *Harvard Medical School*
Kevin T. Beier, *Harvard Medical School*
Claudio Punzo, *Harvard Medical School*
Jeffrey M. Trimarchi, *Harvard Medical School*, et al.

Transcription factor *Olig2* defines subpopulations of retinal progenitor cells biased toward specific cell fates

Brian P. Hafler[a,b,c,1,2], Natalia Surzenko[a,b,c,1], Kevin T. Beier[a,b,c], Claudio Punzo[a,b,c,3], Jeffrey M. Trimarchi[a,b,c,4], Jennifer H. Kong[d], and Constance L. Cepko[a,b,c,5]

[a]Department of Genetics, [b]Department of Ophthalmology, and [c]Howard Hughes Medical Institute, Harvard Medical School, Boston, MA 02115; and [d]Department of Neurobiology, Eli and Edythe Broad Center of Regenerative Medicine and Stem Cell Research, David Geffen School of Medicine at UCLA, Los Angeles, CA 90095

Contributed by Constance L. Cepko, March 9, 2012 (sent for review September 30, 2011)

Previous lineage analyses have shown that retinal progenitor cells (RPCs) are multipotent throughout development, and expression-profiling studies have shown a great deal of molecular heterogeneity among RPCs. To determine if the molecular heterogeneity predicts that an RPC will produce particular types of progeny, clonal lineage analysis was used to investigate the progeny of a subset of RPCs, those that express the basic helix–loop–helix transcription factor, *Olig2*. The embryonic *Olig2*$^+$ RPCs underwent terminal divisions, producing small clones with primarily two of the five cell types being made by the pool of RPCs at that time. The later, postnatal *Olig2*$^+$ RPCs also made terminal divisions, which were biased toward production of rod photoreceptors and amacrine cell interneurons. These data indicate that the multipotent progenitor pool is made up of distinctive types of RPCs, which have biases toward producing subsets of retinal neurons in a terminal division, with the types of neurons produced varying over time. This strategy is similar to that of the developing *Drosophila melanogaster* ventral nerve cord, with the *Olig2*$^+$ cells behaving as ganglion mother cells.

neural progenitors | neural development | oligodendrocyte transcription factor 2

The vertebrate central nervous system (CNS) is composed of a remarkable diversity of cell types. The retina is an accessible region of the CNS and has been studied as a model for the diversification of neuronal cell types. Lineage analyses in several organisms indicate that, during early retinal development, multipotent retinal progenitor cells (RPCs) can give rise to all, or nearly all, of the cell classes (1–6). Lineage analyses of the late RPCs showed clones comprising only a few cells—typically one to three cells—of the late-born cell types (3). Environmental changes (7–9), transplantation experiments (10), and culture of isolated RPCs (11, 12) showed that the production of the temporally appropriate daughter-cell types could occur without the extrinsic cues of neighboring cells. All of these observations suggested that intrinsic properties of RPCs play a major role in directing the fate of the progeny.

Data from a variety of experiments indicate that there are many molecular differences among RPCs (13–17). To reveal this heterogeneity in a comprehensive and high-resolution fashion, we profiled single RPCs across development. Extensive heterogeneity in the expression of many developmental regulators was observed (18). To address whether the molecular heterogeneity among RPCs might correlate with the extensive clonal heterogeneity observed in the previous studies of retrovirally marked clones (3, 4, 19), we used a unique type of retroviral clonal analysis based upon infection of a defined type of RPC. The method relied upon the specific infection of mitotic cells that expressed the *Olig2* basic helix–loop–helix (bHLH) transcription factor. This was achieved by directing infection to those cells in a transgenic mouse line (20) expressing the receptor for an avian virus, tumor virus A (TVA), under the regulation of *Olig2* locus (21). We also used the now classic Cre fate-mapping approach (22) to examine all cells with an *Olig2* expression history.

The findings indicate a model wherein RPCs are functionally and molecularly heterogeneous, thereby providing a basis for the numerous types of clones seen in previous lineage analyses. The findings also provide evidence that some types of RPCs may behave as the ganglion mother cells (GMCs) of the *Drosophila* CNS, as GMCs also make terminal divisions that produce specific types of progeny, which change over time (23–25).

Results

Olig2 Expression in Developing Retina During Embryonic and Postnatal Stages. *Olig2* was previously reported to be expressed in RPCs beginning at embryonic day (E) 12.5, using immunohistochemistry (16, 26, 27). This finding was confirmed by analysis of single-cell transcriptional profiles and in situ hybridization. First, the transcriptomes of 70 single cells harvested from time points between E12.5 to adult were analyzed for *Olig2* expression (Fig. 1*A* and Dataset S1). These cells were analyzed previously (18, 28–31) and classified as RPCs, amacrine cells (ACs), bipolar cells (BPs), photoreceptors (PRs), and Müller glia (MG). *Olig2* was present at a signal level of >1,000 in a small subset of 45 RPCs, but in none of the postmitotic retinal ganglion cells (RGCs), ACs, PRs, BPs and MG.

In situ hybridization was carried out for *Olig2* RNA at different developmental time points. *Olig2* RNA was observed in the outer neuroblastic layer (ONBL), where RPCs reside, at E12.5, E14.5, E16.5, postnatal day (P) 0, P2, and P4 (Fig. 1*B*). In the mature retina, *Olig2* RNA was no longer detected, except in very rare examples of BPs and RGCs. To further investigate if *Olig2* RNA was expressed in mitotic cells, P0 retinas were incubated with [^{3}H]-thymidine for 1 h to label cells in the synthesis (S) phase of the cell cycle and in situ hybridization was performed. At P0, 13% of the [^{3}H]-thymidine–positive cells were *Olig2*$^+$ and 30% of the cells expressing *Olig2* were labeled with [^{3}H]. Because a 1-h labeling period using an S-phase label will only label ~50% of the mitotic cells (32, 33), ~60% of the *Olig2*-expressing cells were mitotic. The remainder were likely cells

Author contributions: C.L.C. designed research; B.P.H., N.S., K.T.B., C.P., J.M.T., and J.H.K. performed research; B.P.H., N.S., and C.L.C. analyzed data; and B.P.H. and C.L.C. wrote the paper.

The authors declare no conflict of interest.

Data deposition: The data for microarrays reported in this paper have been deposited in the Gene Expression Omnibus (GEO) database, www.ncbi.nlm.nih.gov/geo (accession no. GSE37207).

[1]B.P.H. and N.S. contributed equally to this work.

[2]Present address: Department of Ophthalmology and Visual Science, Yale School of Medicine, New Haven, CT 06510.

[3]Present address: Department of Ophthalmology and Gene Therapy Center, University of Massachusetts Medical School, Worcester, MA 01606.

[4]Present address: Department of Genetics, Development and Cell Biology, Iowa State University, Ames, IA 50011.

[5]To whom correspondence should be addressed. E-mail: cepko@genetics.med.harvard.edu.

This article contains supporting information online at www.pnas.org/lookup/suppl/doi:10.1073/pnas.1203138109/-/DCSupplemental.

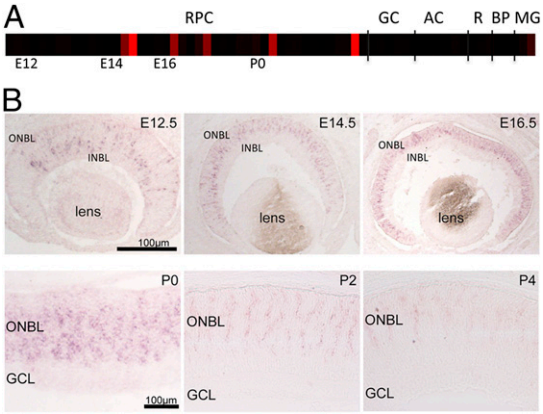

Fig. 1. *Olig2* is expressed by a subset of RPCs. (*A*) Microarray analyses using Affymetrix were conducted on 90 single retinal cells. The values for *Olig2* in each single cell are shown as a heat map, with a value of >2,000 as the maximum intensity color and all other values scaled linearly. The RPCs were taken from across development, beginning at E12 and ending with P5, and examples of other retinal cell types are shown for comparison. Values are given in Dataset S1. Values were taken from refs. 18, 28, 30, and 31. (*B*) In situ hybridization was carried out for *Olig2* probe at the indicated ages. The neuroblastic layer (NBL) and outer neuroblastic layer (ONBL) are the location of RPCs, with the inner neuroblastic layer (INBL) the location of differentiating neurons.

that had recently exited the cell cycle, given the patterns seen by in situ hybridization and on the microarray.

Cre Fate-Mapping of Cells with an Olig2$^+$ History. To determine which retinal cells had an *Olig2* expression history, two lines of knock-in mice with Cre under control of the *Olig2* locus were used. *Olig2-tva-ires-cre*$^{+/-}$ (20) and *Olig2-cre*$^{+/-}$ (34) mice were crossed with several lines of Cre-responsive reporter mice. The results of the cross of *Olig2-cre*$^{+/-}$ to the Cre-sensitive tdTomato reporter line, *Ai9* (35), are shown in Fig. 2. tdTomato expression was seen primarily in the outer nuclear layer and inner nuclear layer (Fig. 2 *A*–*G*). Quantification of the distribution of tdTomato$^+$ cells showed that PRs were the most frequently marked cell type (Fig. 2*H*). There was also an enrichment for ACs and horizontal cells (HCs), compared with overall frequency of ACs and HCs in the retina. BPs were underrepresented among the cells with an *Olig2* history, and tdTomato$^+$ cells were almost never found to express p27^{Kip1} (a marker for MG) (Fig. 2*C*) or Brn3a (a marker for RGCs) (Fig. 2*F* and Fig. S1). When the percentage of the different retinal cell types with *Olig2* expression history was examined, it was clear that majority of ACs, PRs, and HCs had an *Olig2* history (Fig. 2*I*). Additional crosses were made of the *Olig2-tva-ires-cre*$^{+/-}$ line to *Ai9* (Fig. S1), or to *RC::ePE*, which expresses enhanced GFP (eGFP) (36), or to Rosa26R, which expresses LacZ (37). The same pattern of labeling was noted in retinas from these crosses as was seen for the *Olig2-cre*$^{+/-}$*;Ai9* retinas.

Clones Derived from Postnatal Olig2$^+$ RPCs. The Cre fate-mapping studies suggested that *Olig2*$^+$ RPCs produced a particular set of daughter-cell types. However, there was a caveat in this interpretation, as newly postmitotic cells might express *Olig2* transiently, regardless of whether their mitotic RPC expressed *Olig2*. Because the TVA gene was also in the *Olig2* locus, there was an opportunity to examine the descendents only of *Olig2*-expressing RPCs. Retroviral vectors of the type that can only integrate their DNA in mitotic cells (38) can be used to mark TVA$^+$ RPCs and their progeny. Murine cells are only infectable with retroviruses carrying the avian leukosis virus EnvA protein in the viral envelope if they express TVA. The results of infection of *Olig2*$^+$ RPC were compared with the results from infection with a virus with the vesicular stomatitis virus (VSV)-G glycoprotein on its surface, which can infect any mitotic RPC.

Retinas of P0 and P3 *Olig2-tva-ires-cre*$^{+/-}$ mice were infected in vivo with murine retroviruses expressing the marker genes, human placental alkaline phosphatase (AP) (LIA virus) or GFP (pQCXIX-GFP virus). The number of cells, as well as the identity of each cell, was recorded for each clone. Retinas from mice that did not have the TVA gene showed no infection with the EnvA viruses, in keeping with our previous studies (39).

Retinal cell types can be easily classified based upon their locations and their distinctive morphologies. In accord with our previous lineage analyses using retroviruses that can infect any mitotic cell, four cell types were labeled: rod PRs, BPs, ACs, and MGs (Fig. 3, Table 1, and Dataset S2). Labeled cells were arranged in radial clusters, shown to be clones in previous studies (1, 3, 19, 40). The overall frequencies of cell types present in clones derived from P0 *Olig2*$^+$ RPCs were skewed from the control set, with enrichment for rod PRs and ACs. Almost no MG were seen, in keeping with the results from the Cre fate-

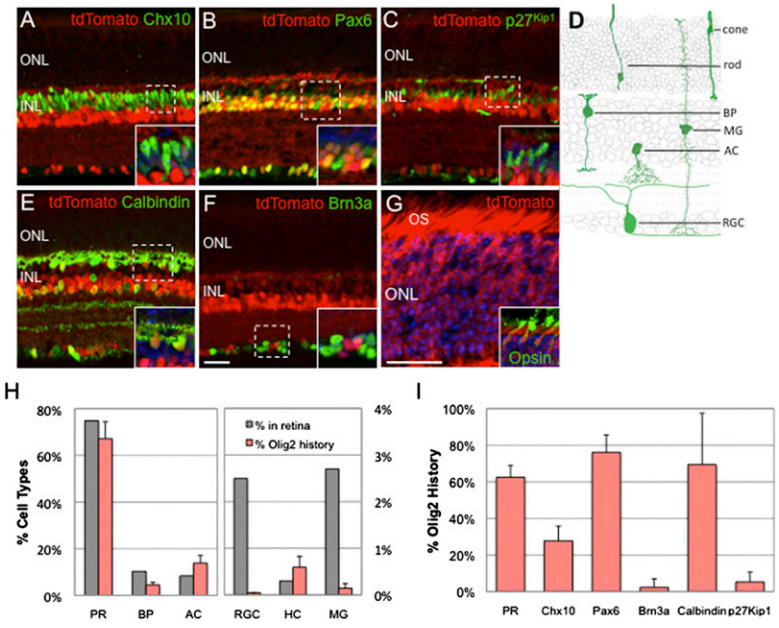

Fig. 2. *Olig2* expression history in the retina was analyzed by crossing an *Olig2* knock-in mouse strain (*Olig2-Cre*$^{+/-}$) (34) to a conditional tdTomato reporter strain (*Ai9*) (35). (*A*–*C and E*–*G*) Expression patterns of the reporter, tdTomato (red), and indicated cell type-specific markers (green) were compared at P20 using immunohistochemistry. Projected image stacks and single confocal plane images of regions labeled with dotted lines (*Insets*) are shown. (*D*) Drawing indicating the locations of the different retinal cell types within the retinal laminae. (*H*) Distribution of cells with *Olig2-Cre* expression history across distinct retinal cell types was quantified on image stacks (40X, 212 × 212 μm) collected from three independent retinas (red bars). The average percentage and SD of tdTomato$^+$ cells that became each of the retinal cell types are shown. The overall frequency of each cell type in the mature retina is shown for comparison (gray bars) (41). (*I*) The percentage of each cell type with *Olig2-cre* expression history, as assessed by immunohistochemistry with the indicated markers, was quantified on image stacks collected from three independent retinas. The frequency of tdTomato$^+$ photoreceptors was calculated as the percentage of outer nuclear layer (ONL) nuclei. OS, outer segements. (Scale bars, 32 μm.)

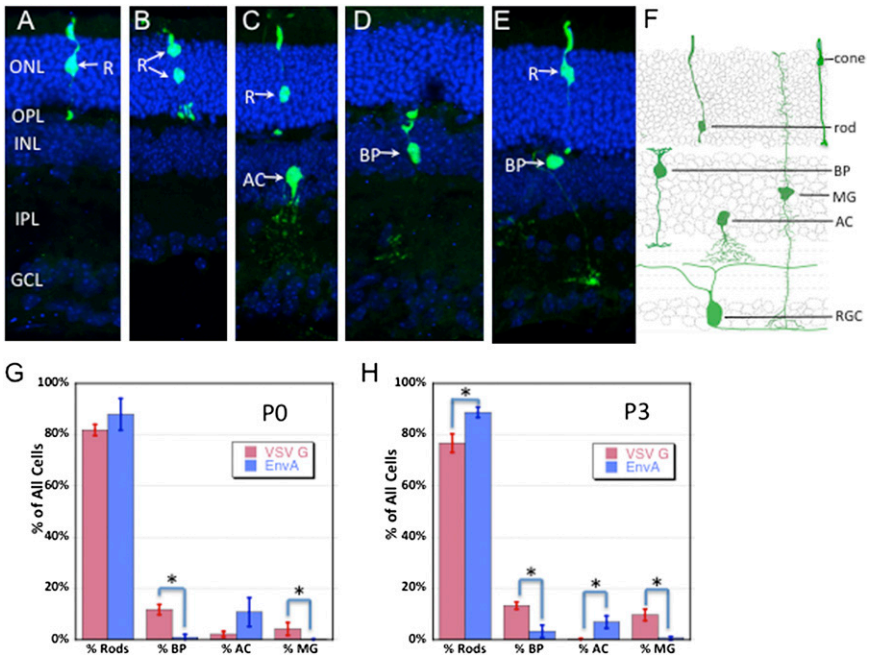

Fig. 3. Morphology and composition of clones following postnatal infection of littermates of *Olig2-tva-ires-cre*$^{+/-}$ retinas with a virus using the EnvA protein or a control virus using the VSV-G envelope protein. Infection was carried out in vivo at P0 or P3 and analysis was carried out >P21. (*A–E*) Micrographs of clones generated by infection of *Olig2-tva-ires-cre*$^{+/-}$ at P3 using GFP retrovirus with EnvA, with each panel depicting a clone type. (*F*) A drawing of the retina, with examples of different cell types. (*G* and *H*) Quantification of all postnatally generated clones was carried out for multiple retinas. The overall frequency of each cell type across all clones are shown for P0 (*G*) and P3 (*H*) infections and comparisons were made for each cell type's frequencies between EnvA and VSV-G infections using the unpaired Student *t* test. *P <0.05. (See also Table 1 and Dataset S2). GCL, ganglion cell layer; IPL, inner plexiform layer; OPL, outer plexiform layer; R, rod photoreceptor. (Magnification: 40× in *A–E*.)

mapping, and few BPs were seen. In addition, there was an enrichment for one- and two-cell clones, with the average clone size being 1.1 ± 0.03 cells per clone for the EnvA clones and 1.43 ± 0.12 for the VSV-G clones (P = 0.0096). No clones of more than two cells were seen in the EnvA dataset, whereas 9.3 ± 5.5% of all clones from VSV-G viruses were more than two cells.

The composition of the one- and two-cell clones derived from the *Olig2*+ P0 RPCs were compared with those of the one- and two-cell control clones. The two-cell clones were skewed toward the rod plus AC composition, with fewer rod PRs plus BP clones relative to the control set. The remainder of the two-cell clones from the *Olig2*$^+$ P0 RPC were almost entirely two rods, and no rod and MG clones were observed from the *Olig2*$^+$ RPCs. Some very unusual two-cell clones of two AC were seen from the *Olig2*$^+$ P0 RPCs, but none were seen in the control set, and very rarely have they been seen in previous lineage studies (3, 40).

Because very few BP cells were seen among the P0 *Olig2*$^+$ RPC descendants, and almost no MG were seen, it was of interest to determine if later *Olig2*$^+$ RPCs might make these cell types. BP and MG have their peak of production later, at approximately P4–P5 (41). Infections were thus carried out at P3. Clones again were compared between the *Olig2*$^+$ RPCs and the controls. A greater number of BP was seen from the P3 *Olig2*$^+$ RPCs (3.3 ± 2.4%) than was seen from the P0 *Olig2*$^+$ RPCs (1.1 ± 1%), but this was significantly lower than that seen in the P3 control set (13.3 ± 1.3%) (P = 0.0013). Again, fewer MG were seen among the *Olig2*$^+$ RPC descendents, and there was a large skew toward ACs (6.89 ± 2.44 from the *Olig2*$^+$ RPCs vs. 0.18 ± 0.32 from the control RPCs, P = 0.006).

Table 1. Clone size and cell type frequencies from postnatal infection

Age	Virus	Total clones	Clone size	% Rod	% BP	% AC	% MG
P0	G	429	AVG 1.43	81.8	11.8	2.2	4.23
			SD 0.12	2.17	2	1.1	2.48
P0	EnvA	510	AVG 1.1	87.9	1	10.8	0.1
			SD 0.03	6.2	1.1	5.6	0.2
			P value 0.0096	0.1800	0.0012	0.0590	0.0455
P3	G	1,000	AVG 1.23	76.7	13.3	0.18	9.7
			SD 0.03	3.6	1.4	0.32	2.2
P3	EnvA		AVG 1.2	88.7	3.3	6.9	0.66
		882	SD 0.09	2	2.4	2.4	0.6
			P value 0.63	0.0024	0.0013	0.0058	0.0004

Composition and distribution of clones following postnatal infection of *Olig2-tva-ires-cre*$^{+/-}$ retinas with LIA virus or pQXIX-GFP virus, with either the EnvA or the VSV-G envelope proteins. Infection was carried out in vivo and retinas were analyzed at maturity (>P21). Quantification and classification of all clones from multiple retinas are in Dataset S2. The average and SD (AVG and SD) for each group are shown, with the Student's two-tailed unpaired *t* test used to calculate *P* values for the indicated comparisons.

Clones Derived from the E13.5 Olig2$^+$ RPCs. To discover the types of progeny made by *Olig2*$^+$ embryonic RPCs, the LIA virus with EnvA was delivered subretinally at E13.5, using ultrasound-guided injections in utero. A previous lineage study was done at E13.5 and E14.5 using a virus that could infect any mitotic cell providing a quantified set of control clones for comparison (4). This study showed that clones comprised radial columns with many cell types, and ranged from 1 to >200 cells. To confirm that the current study could produce similar clones, some retinas were infected with a LIA virus carrying VSV-G in the envelope. These control infections showed large and complex radial clones (Fig. 4*E*). In contrast, when the *Olig2*$^+$ RPCs were targeted at E13.5 using the EnvA virus, the majority of clones were only one or two cells (Fig. 4 *A–D*, Table 2, and Tables S1 and S2). The average clone size from the E13.5 plus E14.5 controls was 32 cells per clone. χ^2 analysis showed a significant difference in the clone sizes between the control and *Olig2*-RPC–derived clones (P value <<001) (Table S1).

The composition of the clones derived from embryonic *Olig2*$^+$ RPC was heavily skewed. Cones comprised only 1.5%, and HC 0.08%, of all cells generated by the control RPCs from E13.5 and E14.5 (Table 2) (4). Cones were 63.8% and HC were 34.1% among the progeny of *Olig2*$^+$ E13.5 RPC. Analysis of the composition of the one-cell clones from *Olig2* RPCs vs. the one-cell clones in the control set showed a very heavy skew toward HCs, and away from the other cell types, other than cones (Fig. 4*G* and Table S2) (P value <<0.001). The composition of two-cell clones showed that the E13.5 *Olig2*$^+$ RPC that gave rise to at least one mitotic daughter gave rise to a mitotic daughter that made clones of one cone and one HC (59%), two HC (15%), two cones (19%), and rarely, one cone and one AC (7%). These clone types were either very rare or not observed among the control set, because very few two-cell clones were seen in the control set.

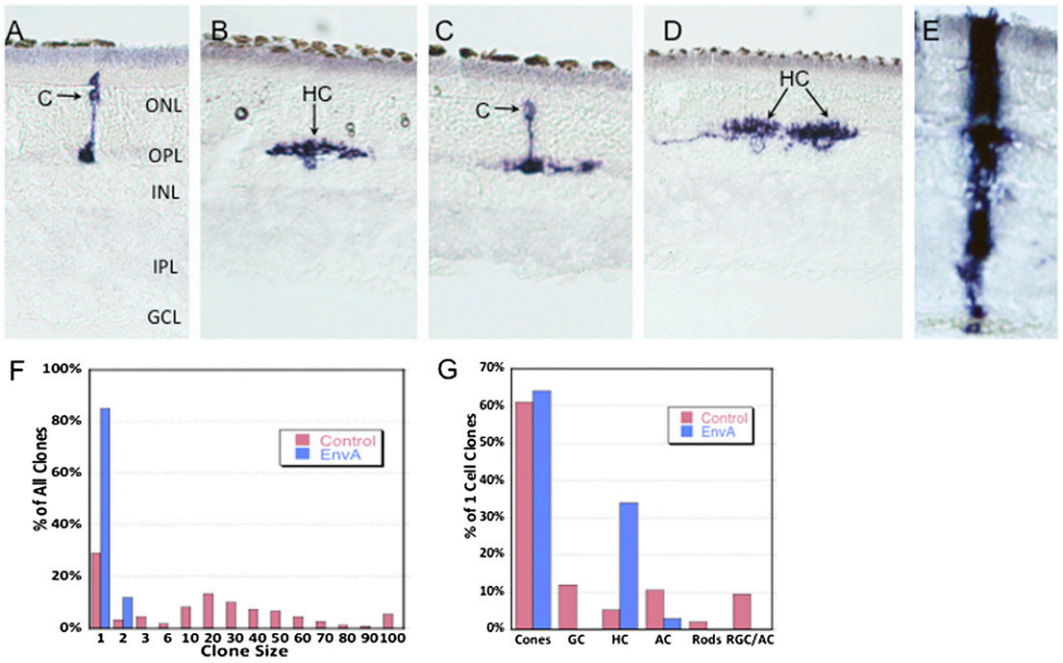

Fig. 4. Clones generated by infection of embryonic *Olig2-tva-ires-cre*$^{+/-}$ retinas with an LIA retrovirus using the EnvA protein. Infection was at E13.5 via ultrasound-guided injections and analysis was conducted >P21. Clones from EnvA (*A*–*D*) were almost entirely one or two cells; those from a control virus were significantly larger (*E*) and resembled those published previously (4). (*F*) The distribution of clone sizes following infection with EnvA or the control virus are shown. (*G*) The frequency of one-cell clone types for EnvA or control virus infection are shown. (See also Table 2 and Table S1.) (Magnification: 40× in *A*–*E*.)

Gene-Expression Differences Among Olig2$^+$ RPCs. Because there were differences among the clone types derived from E13.5 *Olig2*$^+$ RPCs (e.g., either two cones, two HCs, or one cone and one HC) it was of interest to see if there was molecular heterogeneity among *Olig2*$^+$ RPCs, which might correlate with the production of these different clone types. The single-cell RNA profiles of *Olig2*$^+$ cells were thus examined. As *Olig2* is a member of the Clade E bHLH family of genes, and the Clade A bHLH genes are important in neural development, expression of these genes is shown (Fig. 5 and Table S3). *Olig*1 and *bHLHb5*, two other members of Clade E, showed expression in two *Olig2*$^+$ RPCs. The Clade A genes were present in many more cells, with a variety of patterns, in keeping with what has also been seen with immunohistochemical analyses (e.g., ref. 26). Many other types of genes also showed variation across the group of *Olig2*$^+$ RPCs.

Table 2. E13.5 clone types from EnvA infections

Clone type	No. of clones EnvA	Fraction EnvA	No. of clones Control	Fraction Control
1C	119	0.57	58	0.018
2C	5	0.02	2	0.01
1HC	56	0.27	5	0.02
2HC	4	0.02	0	0.00
1C + 1HC	16	0.08	1	0.003
2C + 2HC	2	0.01	0	0.00
1A	5	0.02	10	0.03
1C + 1AC	2	0.01	2	0.06
Total clones* (all types)	209		315	
Overall %C	63.8		1.51	
Overall %HC	34.1		0.08	
Overall %AC	2.9		3.00	

Composition and size of clones generated by infection of E13.5 *Olig2-tva-cre*$^{+/-}$ retinas with LIA retrovirus with the EnvA envelope protein targeting TVA cells. Infection was at E13.5 using ultrasound-guided injections and analysis was conducted after P21. All clones from EnvA infections are shown, and are compared with the frequency of the same clone types from the control viral infections done at E13.5 and E14.5 (4). C, cone cell.
*Two clones of multiple cells were also seen, but could not be analyzed because of dense AP stain.

Olig2 Overexpression in RPCs Promotes Cell Cycle Exit. To address the question of whether *Olig2* can drive cells to exit the cell cycle, *Olig2* was delivered to retinal cells at P0 in vivo using electroporation (42). Twenty-four hours after electroporation, retinas were removed from the animal and cells in S-phase were immediately labeled with a 1-h pulse of EdU (43). The number of electropoorated (GFP$^+$) cells that were also EdU$^+$ was quantified using confocal imaging of retinal sections. In the control, 10.0 ± 2.0% of GFP$^+$ cells were EdU$^+$ (Fig. S2). The number of GFP$^+$ cells that were EdU$^+$ when coelectroporated with *Olig2* was greatly diminished, because only 1.0 ± 1.0% were EdU$^+$, to give a Student *t* test *P* value of 2.45E-4.

Discussion

The development of a complex tissue requires the orchestrated production of a variety of cell types, typically in a temporal order, from pools of progenitor cells. Clonal analyses in the retina have shown that RPCs are multipotent throughout development, with many types of clones produced, even when marking is initiated at a single time point. This complexity led to the question of whether there were different types of RPCs, each dedicated to making particular combinations of progeny. The classic method of Cre fate-mapping used here showed a history of *Olig2* expression primarily within rod PRs, cone PRs, ACs, and HCs. Viral clonal analysis of Olig2$^+$ RPCs showed labeling of the same types of cells. However, the clonal analysis revealed additional aspects of the RPCs that express *Olig2*. Not only did the viral labeling identify clones, as Cre fate-mapping does not, but it avoided the confounding problem of classic Cre fate-mapping wherein all types of cells with Cre-expression history are lumped together.

Olig2$^+$ RPC Are Poised to Make Specific Combinations of Postmitotic Daughter Cells in Terminal Divisions. The current study shows that the bHLH transcription factor, *Olig2*, marks a subpopulation of

RPCs that are biased toward the production of postmitotic progeny. This finding was particularly striking at embryonic time points, when almost every clone from an *Olig2*$^+$ RPC was only one or two cells. This finding means that the embryonic *Olig2*$^+$ RPCs make terminal divisions, and that they do not make the later *Olig2*-expressing RPC. It should be noted that other RPCs, which do not express *Olig2*, also are making terminal divisions at each time when these infections were carried out. This process is indicated by the fact that RGCs are made at E13.5, but very few were marked as having an *Olig2* expression history, and MG and BP cells are made at P0 and P3, but very few came from an Olig2$^+$ RPC.

The observations made here are consistent with those recently reported for expression analysis and fate-mapping of several types of mouse RPCs. Cre fate-mapping of cells with a history of *Atoh7* expression showed a restriction in the types of cells labeled, as they did not include MG or BPs (44, 45). It is not clear how to interpret these findings relative to different types of RPCs, however, as *Atoh7* was reported to not be expressed in cycling cells (44). Brzezkinski et al. also characterized cells with a history of *Ascl1* expression and of *Ngn2* expression (26). These cells included descendents of RPCs that expressed *Ascl1* or *Ngn2*, but also, as pointed out by Brzezkinski et al., cells that expressed these genes as postmitotic cells. Nonetheless, their data are consistent with those shown here; for example, *Ngn2* fate-mapped cells were found in smaller clusters than the retroviral clones mapped from embryonic time points (4). Clonal resolution of the descendents of the *Ngn2*- and *Ascl1*-expressing RPCs will clarify the lineage tree among these types of RPCs and the Olig2$^+$ RPCs.

Olig2 Is a Protein with Multiple Functions. *Olig2* was first shown to be required for the production of motor neurons and oligodendrocytes (46, 47). Subsequently, it has been shown to have several additional roles (48), which are dependent upon its phosphorylation status, which regulates its interaction with different partners. Of note is the role of *Olig2* in inhibiting the cell cycle, as its expression in RPCs correlated with very limited proliferation. In addition, misexpression of *Olig2* drove nearly all of the RPCs out of cell cycle. However, it appears that *Olig2* does not have a major role in regulating retinal development. We examined homozygotes of the *Olig2-tva-ires-cre* knock-in strain for changes in cell types and retinal size. There were no obvious changes in retinal size, nor cell classes, although a thorough analysis of all types of neurons was not done. The overlapping expression of other bHLH genes (Fig. 5) provides a possible explanation, because these genes might have redundant roles with *Olig2*. The presence of the bHLH gene, *Ngn2*, in some *Olig2*-expressing cells is also of interest because it can partner with *Olig2* elsewhere in the CNS (49). A role for *Olig2* in cell-fate decisions will require more precise analyses of gain- and loss-of-function experiments, likely in conjuction with manipulations of other bHLH genes.

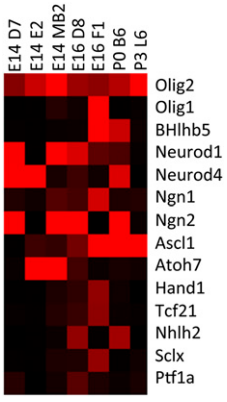

Fig. 5. Heat map showing expression of bHLH genes in individual cells that express *Olig2*. The *Olig2* gene and other members of its bHLH Clade E (56) as well as members of bHLH Clade A are shown. All members of these clades with a value of 1,000 in at least one of these cells are shown. Bright red is a signal value of >2,000 and all other values are scaled from 0 to 2,000. Values were taken from the *Olig2*$^+$ subset of cells listed in Dataset S1 and shown in Fig. 1. The values for this figure are shown in Table S2.

Vertebrate Retinal Development May Use a Strategy Similar to *Drosophila*. The observation of distinct clone types made by *Olig2*$^+$ RPCs in terminal divisions is reminiscent of the strategy used during *Drosophila* ventral nerve cord development. *Drosophila* neuroblasts are neurepithelial cells that exhibit temporal and stereotypical changes in gene expression (24). The vertebrate RPCs also exhibit temporal changes in gene expression, including in gene classes that overlap with those that are temporally regulated in *Drosophila* (17, 18, 26, 50–52). *Drosophila* neuroblasts, which can have extensive proliferation potential, produce GMCs, which have limited proliferation potential because they typically undergo a terminal division. The products of these terminal divisions can be one or two types of cells, and the types that are made are distinct for each type of GMC. The *Olig2*$^+$ clones observed here exhibit the same behavior as the GMCs. (Fig. 6). The clones make terminal divisions and make different clone types over time. Interestingly, the clone types produced at E13.5 included HC-only clones. This is an intriguing observation because previous studies in the chick (19) and zebrafish (53) demonstrated that there was a HC-only RPC. In the chick, which has three types of HC (H1, H2, and H3), a terminal division not only produced two HC, but would make two HC of the same type, either two H1 cells or two H3 cells. This process did not extend to the H2 type, which was not produced in pairs. These data imply that some vertebrate retinal RPCs, perhaps acting as GMCs, are very specifically programmed to not only make a class of retinal neuron, but to make a very specific type. Given the fact that there are >60 types of retinal neurons, this finding implies that there may be a large number of RPC types, which is in keeping with the data on gene expression in single RPCs (18). The RPCs must include neuroblast types of RPC, which give rise to the larger and highly variable types of clones marked at early embryonic times. These RPCs also may be intrinsically programmed to make a series of specific GMCs. Further work to elucidate the patterns of cell division and cell-fate production over time in relation to gene-expression patterns will allow this model to be further evaluated.

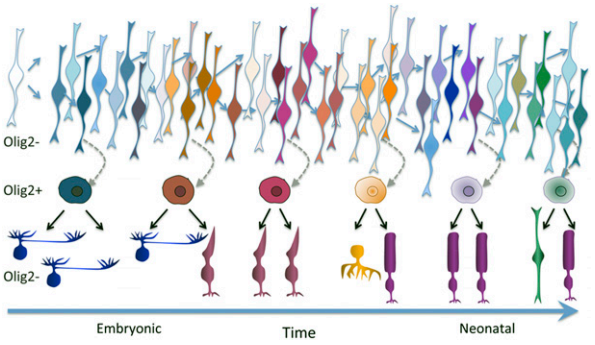

Fig. 6. A model of the progression of RPCs over time. RPCs are able to proliferate to produce very large clones of hundreds to thousands of cells when randomly marked very early in retinal development. *Olig2*-expressing RPCs divide only once to produce two neurons, even early in development. The type of neurons produced by the *Olig2*-expressing RPCs varies over time, as indicated. The terminal divisions and the production of varied types of daughters is a behavior similar to that of the GMCs in the *Drosophila* ventral nerve cord. The model also represents the behavior of the more proliferative RPCs (shown, *Upper*). These cells also vary over time in terms of gene expression and have variable division patterns. The cells may also have programs of gene expression that direct them to make larger clones of particular daughter cell types, as yet undiscovered. Although not shown here, there are *Olig2*$^-$ RPCs that also make terminal divisions (e.g., those that make clones of MG and rods in the neonatal period).

Materials and Methods

Mouse Strains. Previously described strains were used in this study: *Olig2-tva-ires-cre,* provided by David Rowitch (University of California, San Francisco, CA) (20), *Chx10-Cre* (54), *RC::ePE*, provided by Susan Dymecki (Harvard Medical School, Boston, MA) (36), R26R, from Jackson Laboratories (37), Ai9 from Jackson Laboratories (35), and *Olig2*-Cre (34), provided by Ben Novitch (University of California, Los Angeles, CA). All of the animal experiments were approved by the Institutional Animal Care and Use Committee at Harvard University.

In Situ Hybridization and Immunohistochemistry. Protocols can be found in *SI Materials and Methods*.

In Vivo Electroporation of Mouse Retina. Detailed information can be found in *SI Materials and Methods*.

In Vivo Virus Infection and Clonal Analysis. LIA (55) and pQCXIX (Clontech) retroviruses were used in this study. Additional information can be found in *SI Materials and Methods*.

ACKNOWLEDGMENTS. We thank David Rowitch for the gift of the *Olig2-tva-ires-cre* mouse strain; Susan Dymecki for the *RC::*ePE mouse strain; Ben Novitch for the *Olig*2-Cre line; and John Aach, Krista Grande, and Botond Roska for helpful discussions of the statistical analyses. This work was supported by the Howard Hughes Medical Institute (C.L.C. and B.P.H.), Grant NS068012-01 (to K.T.B.), and National Institutes of Health Grant EY008064 (to J.M.T. and N.S.).

1. Fekete DM, Perez-Miguelsanz J, Ryder EF, Cepko CL (1994) Clonal analysis in the chicken retina reveals tangential dispersion of clonally related cells. *Dev Biol* 166: 666–682.
2. Holt CE, Bertsch TW, Ellis HM, Harris WA (1988) Cellular determination in the *Xenopus* retina is independent of lineage and birth date. *Neuron* 1:15–26.
3. Turner DL, Cepko CL (1987) A common progenitor for neurons and glia persists in rat retina late in development. *Nature* 328:131–136.
4. Turner DL, Snyder EY, Cepko CL (1990) Lineage-independent determination of cell type in the embryonic mouse retina. *Neuron* 4:833–845.
5. Wetts R, Fraser SE (1988) Multipotent precursors can give rise to all major cell types of the frog retina. *Science* 239:1142–1145.
6. Wong LL, Rapaport DH (2009) Defining retinal progenitor cell competence in *Xenopus laevis* by clonal analysis. *Development* 136:1707–1715.
7. Belliveau MJ, Cepko CL (1999) Extrinsic and intrinsic factors control the genesis of amacrine and cone cells in the rat retina. *Development* 126:555–566.
8. Belliveau MJ, Young TL, Cepko CL (2000) Late retinal progenitor cells show intrinsic limitations in the production of cell types and the kinetics of opsin synthesis. *J Neurosci* 20:2247–2254.
9. Morrow EM, Belliveau MJ, Cepko CL (1998) Two phases of rod photoreceptor differentiation during rat retinal development. *J Neurosci* 18:3738–3748.
10. Kay JN, Link BA, Baier H (2005) Staggered cell-intrinsic timing of ath5 expression underlies the wave of ganglion cell neurogenesis in the zebrafish retina. *Development* 132:2573–2585.
11. Cayouette M, Barres BA, Raff M (2003) Importance of intrinsic mechanisms in cell fate decisions in the developing rat retina. *Neuron* 40:897–904.
12. Gomes FL, et al. (2011) Reconstruction of rat retinal progenitor cell lineages in vitro reveals a surprising degree of stochasticity in cell fate decisions. *Development* 138: 227–235.
13. Guillemot F, Joyner AL (1993) Dynamic expression of the murine Achaete-Scute homologue Mash-1 in the developing nervous system. *Mech Dev* 42:171–185.
14. Jasoni CL, Reh TA (1996) Temporal and spatial pattern of MASH-1 expression in the developing rat retina demonstrates progenitor cell heterogeneity. *J Comp Neurol* 369:319–327.
15. Li S, et al. (2004) Foxn4 controls the genesis of amacrine and horizontal cells by retinal progenitors. *Neuron* 43:795–807.
16. Nakamura K, Harada C, Namekata K, Harada T (2006) Expression of olig2 in retinal progenitor cells. *Neuroreport* 17:345–349.
17. Blackshaw S, et al. (2004) Genomic analysis of mouse retinal development. *PLoS Biol* 2: E247.
18. Trimarchi JM, Stadler MB, Cepko CL (2008) Individual retinal progenitor cells display extensive heterogeneity of gene expression. *PloS One* 3:e1588.
19. Rompani SB, Cepko CL (2008) Retinal progenitor cells can produce restricted subsets of horizontal cells. *Proc Natl Acad Sci USA* 105:192–197.
20. Schüller U, et al. (2008) Acquisition of granule neuron precursor identity is a critical determinant of progenitor cell competence to form Shh-induced medulloblastoma. *Cancer Cell* 14:123–134.
21. Bates P, Rong L, Varmus HE, Young JA, Crittenden LB (1998) Genetic mapping of the cloned subgroup A avian sarcoma and leukosis virus receptor gene to the TVA locus. *J Virol* 72:2505–2508.
22. Branda CS, Dymecki SM (2004) Talking about a revolution: The impact of site-specific recombinases on genetic analyses in mice. *Dev Cell* 6:7–28.
23. Baumgardt M, Miguel-Aliaga I, Karlsson D, Ekman H, Thor S (2007) Specification of neuronal identities by feedforward combinatorial coding. *PLoS Biol* 5:e37.
24. Isshiki T, Pearson B, Holbrook S, Doe CQ (2001) *Drosophila* neuroblasts sequentially express transcription factors which specify the temporal identity of their neuronal progeny. *Cell* 106:511–521.
25. Zhong W (2003) Diversifying neural cells through order of birth and asymmetry of division. *Neuron* 37:11–14.
26. Brzezinski, JA, 4th, Kim EJ, Johnson JE, Reh TA (2011) Ascl1 expression defines a subpopulation of lineage-restricted progenitors in the mammalian retina. *Development* 138:3519–3531.
27. Shibasaki K, Takebayashi H, Ikenaka K, Feng L, Gan L (2007) Expression of the basic helix-loop-factor *Olig2* in the developing retina: *Olig2* as a new marker for retinal progenitors and late-born cells. *Gene Expr Patterns* 7:57–65.
28. Cherry TJ, Trimarchi JM, Stadler MB, Cepko CL (2009) Development and diversification of retinal amacrine interneurons at single cell resolution. *Proc Natl Acad Sci USA* 106: 9495–9500.
29. Kim DS, et al. (2008) Identification of molecular markers of bipolar cells in the murine retina. *J Comp Neurol* 507:1795–1810.
30. Roesch K, et al. (2008) The transcriptome of retinal Müller glial cells. *J Comp Neurol* 509:225–238.
31. Trimarchi JM, et al. (2007) Molecular heterogeneity of developing retinal ganglion and amacrine cells revealed through single cell gene expression profiling. *J Comp Neurol* 502:1047–1065.
32. Young RW (1985) Cell proliferation during postnatal development of the retina in the mouse. *Brain Res* 353:229–239.
33. Alexiades MR, Cepko C (1996) Quantitative analysis of proliferation and cell cycle length during development of the rat retina. *Dev Dyn* 205:293–307.
34. Dessaud E, et al. (2007) Interpretation of the sonic hedgehog morphogen gradient by a temporal adaptation mechanism. *Nature* 450:717–720.
35. Madisen L, et al. (2010) A robust and high-throughput Cre reporting and characterization system for the whole mouse brain. *Nat Neurosci* 13:133–140.
36. Nielsen CM, Dymecki SM (2010) Sonic hedgehog is required for vascular outgrowth in the hindbrain choroid plexus. *Dev Biol* 340:430–437.
37. Soriano P (1999) Generalized lacZ expression with the ROSA26 Cre reporter strain. *Nat Genet* 21:70–71.
38. Roe T, Reynolds TC, Yu G, Brown PO (1993) Integration of murine leukemia virus DNA depends on mitosis. *EMBO J* 12:2099–2108.
39. Beier KT, Samson ME, Matsuda T, Cepko CL (2011) Conditional expression of the TVA receptor allows clonal analysis of descendents from Cre-expressing progenitor cells. *Dev Biol* 353:309–320.
40. Fields-Berry SC, Halliday AL, Cepko CL (1992) A recombinant retrovirus encoding alkaline phosphatase confirms clonal boundary assignment in lineage analysis of murine retina. *Proc Natl Acad Sci USA* 89:693–697.
41. Young RW (1985) Cell differentiation in the retina of the mouse. *Anat Rec* 212: 199–205.
42. Matsuda T, Cepko CL (2004) Electroporation and RNA interference in the rodent retina in vivo and in vitro. *Proc Natl Acad Sci USA* 101:16–22.
43. Salic A, Mitchison TJ (2008) A chemical method for fast and sensitive detection of DNA synthesis in vivo. *Proc Natl Acad Sci USA* 105:2415–2420.
44. Yang Z, Ding K, Pan L, Deng M, Gan L (2003) Math5 determines the competence state of retinal ganglion cell progenitors. *Dev Biol* 264:240–254.
45. Feng L, et al. (2010) MATH5 controls the acquisition of multiple retinal cell fates. *Mol Brain* 3:36.
46. Lu QR, et al. (2002) Common developmental requirement for Olig function indicates a motor neuron/oligodendrocyte connection. *Cell* 109:75–86.
47. Novitch BG, Chen AI, Jessell TM (2001) Coordinate regulation of motor neuron subtype identity and pan-neuronal properties by the bHLH repressor Olig2. *Neuron* 31: 773–789.
48. Gaber ZB, Novitch BG (2011) All the embryo's a stage, and Olig2 in its time plays many parts. *Neuron* 69:833–835.
49. Li H, de Faria JP, Andrew P, Nitarska J, Richardson WD (2011) Phosphorylation regulates OLIG2 cofactor choice and the motor neuron-oligodendrocyte fate switch. *Neuron* 69:918–929.
50. Brzezinski, JA, 4th, Lamba DA, Reh TA (2010) Blimp1 controls photoreceptor versus bipolar cell fate choice during retinal development. *Development* 137:619–629.
51. Elliott J, Jolicoeur C, Ramamurthy V, Cayouette M (2008) Ikaros confers early temporal competence to mouse retinal progenitor cells. *Neuron* 60:26–39.
52. Katoh K, et al. (2010) Blimp1 suppresses Chx10 expression in differentiating retinal photoreceptor precursors to ensure proper photoreceptor development. *J Neurosci* 30:6515–6526.
53. Godinho L, et al. (2007) Nonapical symmetric divisions underlie horizontal cell layer formation in the developing retina in vivo. *Neuron* 56:597–603.
54. Rowan S, Cepko CL (2004) Genetic analysis of the homeodomain transcription factor Chx10 in the retina using a novel multifunctional BAC transgenic mouse reporter. *Dev Biol* 271:388–402.
55. Bao ZZ, Cepko CL (1997) The expression and function of Notch pathway genes in the developing rat eye. *J Neurosci* 17:1425–1434.
56. Skinner MK, Rawls A, Wilson-Rawls J, Roalson EH (2010) Basic helix-loop-helix transcription factor gene family phylogenetics and nomenclature. *Differentiation* 80:1–8.